Eur. Phys. J. B (2022)95:167
https://doi.org/10.1140/epjb/s10051-022-00431-9

THE EUROPEAN PHYSICAL JOURNAL B

Regular Article - Solid State and Materials

Effects of ferromagnetism in ab initio calculations of basic structural parameters of Fe-A (A = Mo, Nb, Ta, V, or W) random binary alloys

Shuozhi Xu[1], Arjun S. Kulathuvayal[2], Liming Xiong[3], and Yanqing Su[2,a]

[1] Department of Mechanical Engineering, University of California, Santa Barbara, CA 93106-5070, USA
[2] Department of Mechanical and Aerospace Engineering, Utah State University, Logan, UT 84322-4130, USA
[3] Department of Aerospace Engineering, Iowa State University, Ames, IA 50011, USA

Received 3 December 2021 / Accepted 29 September 2022

Abstract. Density functional theory (DFT) calculations are performed to study the effects of ferromagnetism on basic structural parameters including lattice parameters and elastic constants in 45 body-centered cubic (BCC) Fe-based random binary alloys. Each binary consists of Fe and one of the five pure BCC metals, including Mo, Nb, Ta, V, and W. To provide references, six pure metals are also studied. It is found that (i) the effects of ferromagnetism are more pronounced for elastic constants than for lattice parameter, (ii) the effects of ferromagnetism increase with the Fe concentration in the binary, (iii) when ferromagnetism is neglected in DFT calculations, pure Fe is elastically unstable, while most Fe-based alloys are stable, and (iv) relatively good estimates of the structural parameters of alloys can be provided via the simple rule of mixtures only when the ferromagnetism is included.

1 Introduction

In crystalline materials, basic structural parameters such as the elastic constants C_{ij} form the base for deriving a series of mechanical properties of these materials, e.g., Cauchy pressure, bulk modulus, Young's modulus, shear modulus, Zener ratio, Pugh ratio, and Poisson's ratio [1,2]. Therefore, it is critical to accurately measure these structural parameters in experiments or calculate them via ab initio methods, such as density functional theory (DFT). In DFT, caution must be taken when the material is of ferromagnetic or antiferromagnetic nature. Prior DFT studies have uncovered effects of magnetism on lattice parameter, cohesive energy, bulk modulus, surface energy, density of states, ground state, Fermi level, and generalized stacking fault energy in Co [3–8], Cr [3,9], Fe [3–6,10–14], Ni [3–6,15], Pu [16,17], oxides [18–20], and metallic alloys [21–25]. Some notable consequences of ignoring ferromagnetism in ab initio calculations are: (i) the ground state of Fe was found to be hexagonal close-packed [5] instead of the correct one: body-centered cubic (BCC); (ii) the tetragonal shear modulus $C' = (C_{11} - C_{12})/2$ is negative in BCC α-Fe [6,26] and face-centered cubic (FCC) δ-Pu [16,17], while it should be positive in both lattices according to experiments [27–29]; and (iii) C_{11} of α-Fe is negative [26], while it is positive according to both experiments [27,28,30] and ferromagnetism-included DFT calculations [6,14,31–33]. The last two results suggest that α-Fe, i.e., BCC Fe, becomes elastically unstable if ferromagnetism is neglected in ab initio calculations.

In this paper, we expand upon prior DFT studies in pure Fe to study the effects of ferromagnetism on calculations of basic structural parameters in 45 Fe-based random binary alloys. Five alloying elements, including Mo, Nb, Ta, V, and W, are considered. Among these elements, only V is soluble in BCC Fe over the entire concentration range within the high-temperature paramagnetic phase [34,35]. Thus, $Fe_{1-x}V_x$ ($x \leq 0.1$) were studied for their basic structural parameters using either DFT calculations [35] or experiments [36]. The solid solubilities of the other four elements in BCC Fe are less than 2.5 at.% at temperatures no higher than 900 °C [34]. Nevertheless, it is of theoretical interest to explore random binary alloys that involve all these alloying elements. Our findings are expected to provide a solid foundation for future studies of ferromagnetism in more complex alloys such as the Fe-based high entropy alloys [1,22,37].

2 Methodology

Special quasi-random structures (SQS) [38] in BCC lattices are built using ATAT [39]. The tolerance for matching correlations of the SQS and of the ideal ran-

[a] e-mail: yanqing.su@usu.edu (corresponding author)

Published online: 12 October 2022

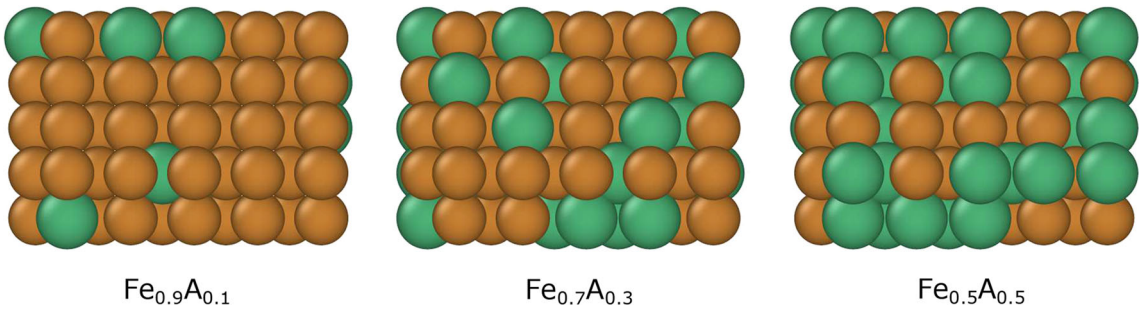

Fig. 1 Atomistic structures of $Fe_{0.9}A_{0.1}$, $Fe_{0.7}A_{0.3}$, and $Fe_{0.5}A_{0.5}$. Brown and green atoms are Fe and A, respectively. Visualization is done in OVITO [42]

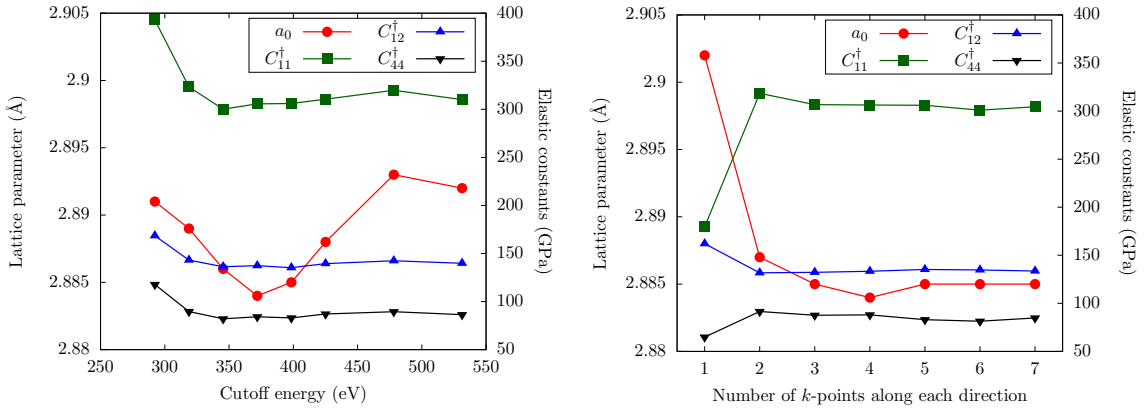

(a) Cutoff energy **(b)** k-point

Fig. 2 Lattice parameter a_0 and elastic constants $C_{ij}^{\dagger}$ in $Fe_{0.5}V_{0.5}$ as a function of **a** the cut-off energy and **b** the number of k-points along each direction. In **a**, a k-point mesh of $5 \times 5 \times 5$ is employed. In **b**, a cut-off energy of 398.52 eV is adopted

dom state is 0.01. A tentative lattice parameter of 3 Å is assumed, because it is close to the experimental lattice parameters of the six pure BCC metals studied here [40]. Both pair and triplet correlation functions are considered, with the ranges being 13 Å and 17 Å, respectively. According to our recent work [41], these two ranges are large enough for the matching correlations of the SQS to converge to that of the ideal random state. Nine SQS are constructed for $Fe_{1-x}A_x$, where x ranges from 0.1 to 0.9, in increment of 0.1. The chemical element A is Mo, Nb, Ta, V, or W. As a result, there are 45 random binary alloys in total.

Each simulation cell is a cuboid containing 80 atoms, with ⟨100⟩ crystallographic orientations along all three directions. The simulation cell contains $4 \times 5 \times 2$ unit cells along the three directions, where each unit cell contains two atoms. Three SQS are shown in Fig. 1. A prior DFT study in an FCC random AlTi binary found that if a randomly generated supercell is too small, there would be too large scatter in the calculated elastic constants; in the meantime, an SQS containing 32 atoms provides the same elastic constants as a random supercell containing up to 4000 atoms [43]. Therefore, our SQS which contains 80 atoms is appropriate.

All DFT calculations are carried out using VASP [44]. Based on the projector augmented wave method [45,46], a plane-wave basis with a cut-off energy of 398.52 eV is adopted. To approximate the exchange-correlation energy functional, the Perdew–Burke–Ernzerhof formulation of the generalized gradient approximation [47] is used. The Brillouin zone is constructed by the Monkhorst–Pack scheme [48], with a smearing width of 0.2 eV based on the Methfessel–Paxton smearing method [49]. The k-point mesh is $5 \times 5 \times 5$. Convergence analyses for the cut-off energy and k-point mesh are presented in Fig. 2. The residual minimization scheme with direct inversion in the iterative subspace is employed for the electronic self-consistent loop; the convergence is reached when the total free energy change between two steps is smaller than 10^{-4} eV [50]. The ionic relaxation stops when the total energy between two steps is smaller than 10^{-3} eV/atom [15]. The relaxation method and the stress–strain method are employed, respectively, to calculate the lattice parameter a_0 and elastic tensor $\boldsymbol{C}$. These two methods were recently shown [41] to yield close results in six pure BCC metals compared with the volume-energy method (for a_0) and the energy-strain method (for $\boldsymbol{C}$), which were used in some prior DFT calculations in BCC Fe [5,6,11,13,14,31,33]. Note that in the relaxation method, the cell volume, but not cell shape, is allowed to relax; for selected binaries, we

Table 1 Lattice parameter a_0 (in Å) and elastic constants C_{11}, C_{12}, C_{44} (in GPa) in six pure BCC metals. All DFT data except those of Fe and Fe^{NM} are from a recent work [41]. The superscript 'NM' denotes results from non-magnetic DFT calculations. All experimental data (Exp) are from Ref. [40]

		Fe	Fe^{NM}	Mo	Nb	Ta	V	W
a_0	DFT	2.842	2.762	3.162	3.322	3.321	2.999	3.184
	Exp	2.867		3.147	3.301	3.303	3.024	3.165
C_{11}	DFT	261.44	53.5	461.39	242.23	258.1	264.61	526.52
	Exp	230		465	245	264	230	523
C_{12}	DFT	135.18	344.09	160.84	134.92	165.11	132.95	199.34
	Exp	135		163	132	158	120	203
C_{44}	DFT	93.63	176.53	102.87	13.76	75.91	24.2	145.39
	Exp	117		109	28.4	82.6	43.1	160

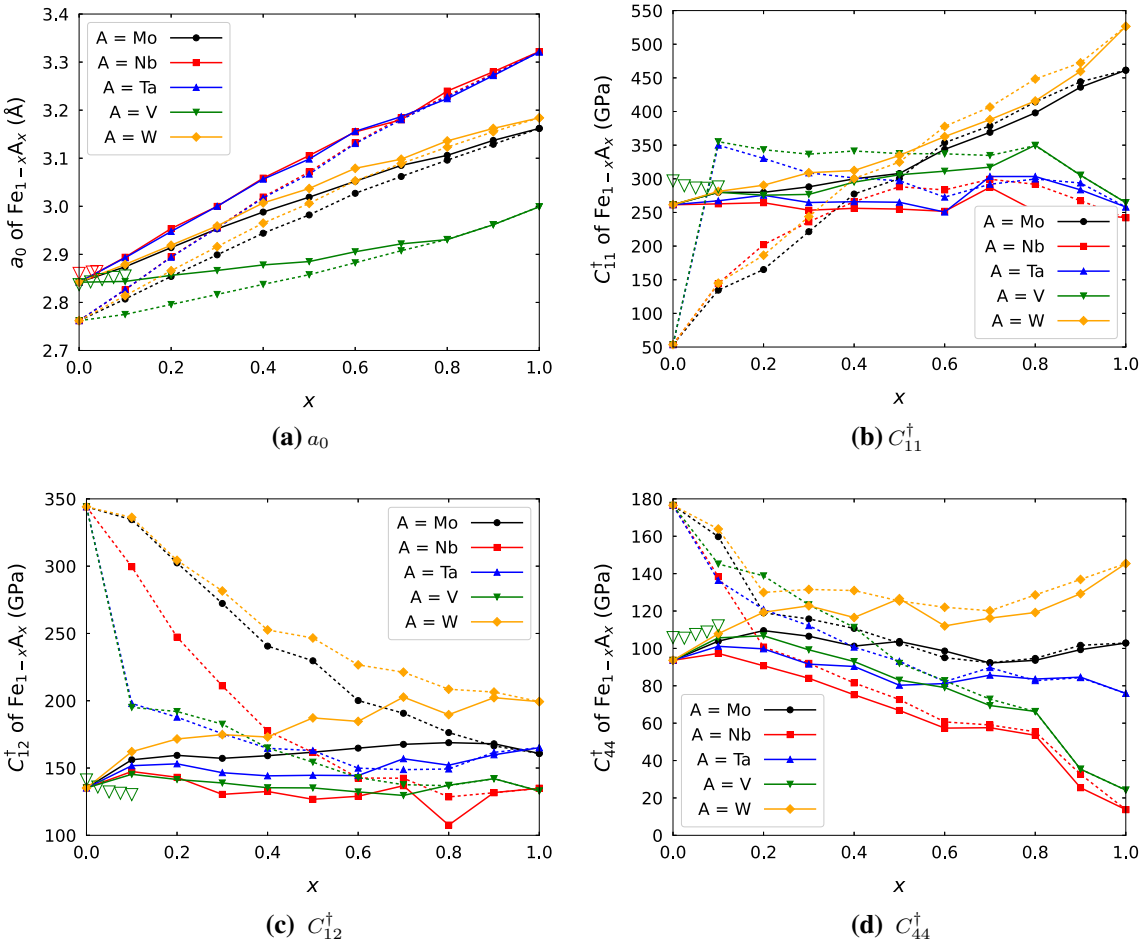

Fig. 3 Lattice parameters a_0 and elastic constants $C_{ij}^{\dagger}$ in six pure metals (when $x = 0$ or 1) and 45 Fe-based random binary alloys (when $0 < x < 1$) based on ferromagnetic (solid lines) and non-magnetic (dashed lines) DFT calculations. Red and green open triangles denote data from prior experiments [36] and DFT calculations [35], respectively, for $Fe_{1-x}V_x$ ($x \leq 0.1$)

conduct relaxation that allow for both cell shape and volume to relax, resulting in very similar (< 0.5% different) lattice parameter. Value of the tentative lattice parameter, i.e., 3 Å, does not affect the final, relaxed lattice parameter, while an appropriate tentative value indeed facilitates the relaxation process. Two sets of DFT calculations are considered for all binary alloys. The first set considers ferromagnetism of the Fe atoms, while the other set does not consider the spin polarization at all, i.e., assuming that Fe is non-magnetic. To complement these results, basic structural parameters of six pure metals—Fe, Mo, Nb, Ta, V, and W—are provided. Data for the last five pure metals are taken from our recent work [9], while those for Fe are newly calculated in this paper, using a simulation cell containing two Fe atoms for which non-magnetism or

ferromagnetism is considered. For pure metals, all DFT parameters are the same as those for alloys, except that a k-point mesh of $11 \times 11 \times 11$ is used instead.

3 Results and discussion

Lattice parameters a_0 and elastic constants C_{11}, C_{12}, and C_{44} in six pure BCC metals are presented in Table 1. DFT data agree with experimental ones [40] relatively well. It is found that Nb and Ta, which are group 5 elements, have the largest a_0, while Fe, which is in group 8, the smallest. On average, W has the largest elastic constants C_{ij}, while Nb the smallest. Non-magnetic calculations in Fe, denoted as Fe^{NM}, yield smaller a_0 and C_{11} as well as larger C_{12} and C_{44}, than ferromagnetic calculations. Prior DFT calculations in Fe also found that neglecting ferromagnetism results in smaller a_0 [5,6,13] and C_{11} [6], as well as larger C_{12} and C_{44} [6], in agreement with our findings.

In a pure metal with a cubic lattice, some elastic constants are non-zero and equal, that is

$$C_{11} = C_{22} = C_{33} \neq 0 \quad (1)$$
$$C_{12} = C_{23} = C_{13} \neq 0 \quad (2)$$
$$C_{44} = C_{55} = C_{66} \neq 0, \quad (3)$$

while all other constants are zero. For such a metal to be elastically stable, all three Born criteria [51] must be satisfied, that is

$$C_{11} - C_{12} > 0;\ C_{11} + 2C_{12} > 0;\ C_{44} > 0. \quad (4)$$

Based on Table 1, the only material that is elastically unstable is Fe^{NM}, for which $C_{11} - C_{12} < 0$, which was also found in prior non-magnetic DFT [6] and tight-binding [26] calculations.

In random alloys, Eqs. 1–3 usually do not hold and elastic constants, such as C_{34}, C_{45}, and C_{56}, are usually not zero. These were previously reported in FCC [25] and BCC [52] random ternary alloys. Following our recent work in BCC multi-principal element alloys [41], we calculate the effective BCC elastic constants in all random binary alloys using the following relationships:

$$C'_{11} = \frac{C_{11} + C_{22} + C_{33}}{3} \quad (5)$$
$$C'_{12} = \frac{C_{12} + C_{13} + C_{23}}{3} \quad (6)$$
$$C'_{44} = \frac{C_{44} + C_{55} + C_{66}}{3}. \quad (7)$$

Values of a_0, C'_{11}, C'_{12}, and C'_{44} in 45 Fe-based random binary alloys are summarized in Fig. 3, as a function of the chemical concentration x. Prior experimental [36] and DFT [35] data for $Fe_{1-x}V_x$ ($x \leq 0.1$) are also presented, and are compared favorably with our DFT results.

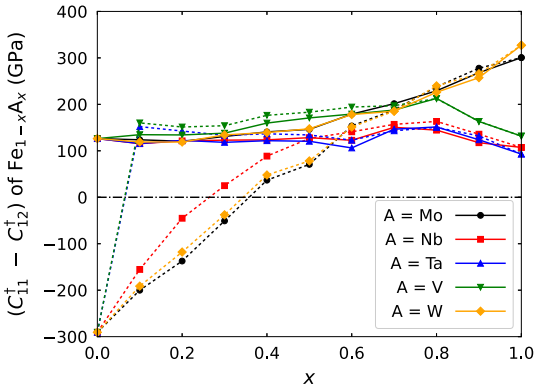

Fig. 4 Difference between C'_{11} and C'_{12} in six pure metals (when $x = 0$ or 1) and 45 Fe-based random binary alloys (when $0 < x < 1$) based on ferromagnetic (solid lines) and non-magnetic (dashed lines) calculations. Above the horizontal dash-dotted line, materials are elastically stable

Since Fe and Fe^{NM} have the smallest a_0 among all pure metals, value of a_0 of $Fe_{1-x}A_x$ or $Fe^{NM}_{1-x}A_x$ is expected to increase with x. Figure 3a confirms this monotonic, near-linear trend, suggesting that a_0 of all alloys may be accurately predicted using the simple rule of mixtures based on a_0 and concentration of constituent metals.

However, the rule of mixtures would not be accurate in predicting C'_{ij} of alloys, although the trend would be correct in most cases, as shown in Fig. 3b–d. For C'_{12}, its value in Fe is close to those in other five pure metals, and C'_{12} of $Fe_{1-x}A_x$ is indeed largely insensitive to x. In the meantime, Fe^{NM} has a much higher C'_{12} than other five pure metals. As a result, C'_{12} of $Fe^{NM}_{1-x}A_x$ generally decreases with an increasing x, albeit not linearly. The variations of C'_{11} and C'_{44} among all alloys are similar to that of C'_{12}, except C'_{11} of $Fe^{NM}_{1-x}Ta_x$ and $Fe^{NM}_{1-x}V_x$. For these two sets of alloys, $Fe^{NM}_{0.9}A_{0.1}$ has a much larger C'_{11} than pure Fe^{NM}; then, as x increases, C'_{11} gradually decreases, until the material becomes pure Ta or pure V.

Taken together, our DFT calculations suggest that the simple rule of mixtures can provide relatively good estimates of a_0 and C'_{ij} when ferromagnetism is considered for Fe atoms but not necessarily so when magnetism is neglected. The latter conclusion holds true for non-magnetic calculations in Cr-based random binary alloys, as shown in Appendix A.

Since pure Fe^{NM} is elastically unstable because of its negative value of $(C_{11} - C_{12})$, it is interesting to assess the elastic stability of $Fe^{NM}_{1-x}A_x$ by substituting the three effective BCC elastic constants into Eq. 4. To this end, values of $(C'_{11} - C'_{12})$ in all pure metals and alloys are plotted as a function of the concentration x in Fig. 4. It is found that most binary alloys are elastically stable except pure Fe^{NM}, $Fe^{NM}_{1-x}Mo_x$ and $Fe^{NM}_{1-x}W_x$ when $x \leq 0.3$, and $Fe^{NM}_{1-x}Nb_x$ when $x \leq 0.2$.

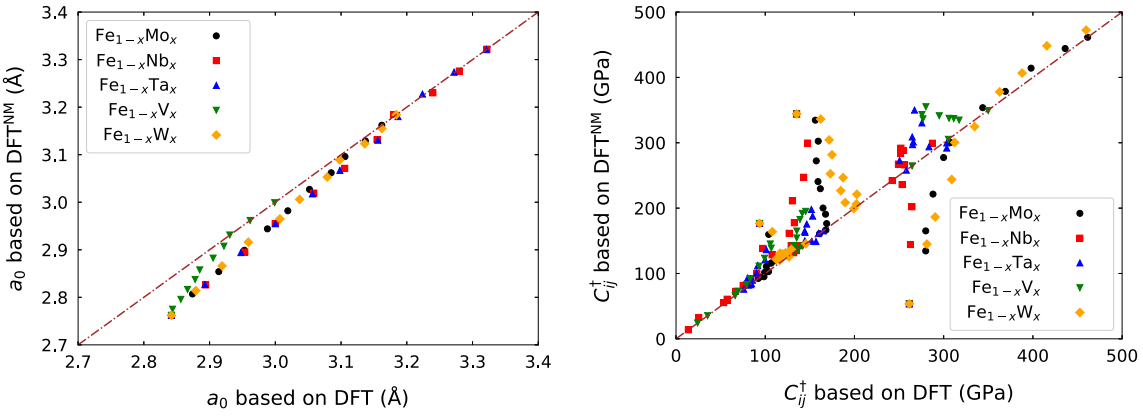

(a) Lattice parameter **(b)** Elastic constants

Fig. 5 **a** Lattice parameters and **b** elastic constants of six pure metals and 45 Fe-based random binary alloys based on DFT calculations with ferromagnetism or without (superscript 'NM')

In the meantime, all $Fe^{NM}_{1-x}Ta_x$ and $Fe^{NM}_{1-x}V_x$ alloys are stable, regardless of x. On the one hand, since all alloying elements are stable, non-magnetic, BCC metals, it is expected that the elastic stability of $Fe^{NM}_{1-x}A_x$ would be gradually improved as a result of the continuous alloying, i.e., as x increases. On the other hand, it is interesting that the effect of elastic instability of pure Fe^{NM} quickly diminishes as its concentration in a binary decreases. As for the $Fe_{1-x}A_x$ alloys, all of them are elastically stable, as expected.

Results so far show pronounced effects of ferromagnetism on basic structural parameters in pure Fe and most Fe-based alloys. To better demonstrate these effects, we present in Fig. 5 comparisons of lattice parameters a_0 and elastic constants $C^{\dagger}_{ij}$ between DFT calculations with ferromagnetism and those without. For a_0, the relative difference is within 3%, and including ferromagnetism into DFT calculations always increases a_0. For $C^{\dagger}_{ij}$, the relative difference is much larger than that in a_0, and the effects of ferromagnetism are more pronounced when Fe concentration is higher (i.e., smaller x). The difference in the ferromagnetism effects between a_0 and $C^{\dagger}_{ij}$ could be due to that the lattice remains largely undistorted in calculating the former, while it must be sufficiently distorted to obtain the latter. Prior experiments [53] and calculations [54] revealed that the magnetic property of a crystal could be strongly influenced by the lattice distortion.

4 Conclusions

In this paper, we calculate basic structural parameters, including lattice parameters and elastic constants in 45 random binary alloys that consist of Fe and one of five BCC metals: Mo, Nb, Ta, V, and W. Two sets of DFT calculations are conducted. The first set considers ferromagnetism of Fe atoms, while the second assumes non-magnetism. It is found that the effects of ferromagnetism are more pronounced for the elastic constants than for the lattice parameter. In binary alloys, the effects of ferromagnetism increase with the Fe concentration. In particular, non-magnetic DFT calculations predict elastically unstable pure Fe, some $Fe_{1-x}Mo_x$, $Fe_{1-x}Nb_x$, and $Fe_{1-x}W_x$, where $x \leq 0.2$–0.3. We also find that the simple rule of mixtures can provide a relatively accurate estimation of structural parameters of alloys only when ferromagnetism is included in DFT calculations.

Acknowledgements We thank Dr. Sai Mu for helpful discussions. The support and resources from the Center for High Performance Computing at the University of Utah are gratefully acknowledged.

Author contributions

SX and YS designed the project. SX conducted all calculations. SX and ASK processed data. LX helped interpret results. SX wrote the paper with input from all other authors.

Data Availability Statement The data that support the findings of this study are available from the corresponding author upon reasonable request. This manuscript has no associated data or the data will not be deposited. [Authors' comment: All results can be replicated using the numerical procedures described in the paper.]

A Non-magnetic DFT calculations in Cr-based random binary alloys

Lattice parameters and elastic constants of 45 Cr-based random binary alloys are calculated using non-magnetic DFT calculations. Simulation details are the same as in Sect. 2. Results are summarized in Fig. 6.

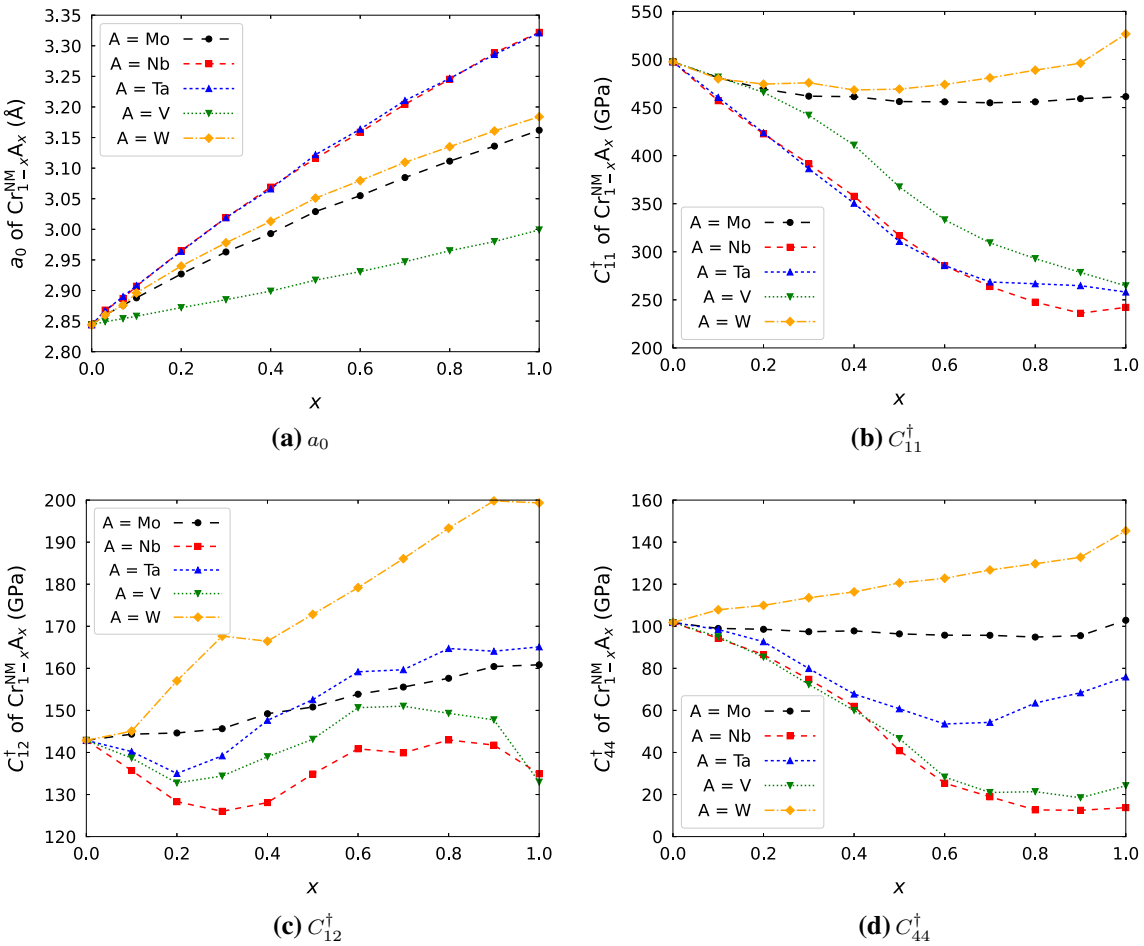

Fig. 6 Lattice parameters a_0 and elastic constants $C_{ij}^{\dagger}$ in six pure metals (when $x = 0$ or 1) and 45 Cr-based random binary alloys (when $0 < x < 1$) based on non-magnetic DFT calculations

References

1. Y. Chen, Q. Zhao, H. Wu, Q. Fang, J. Li, Phys. B Condens. Matter **615**, 413078 (2021)
2. S. Xu, Y. Su, I.J. Beyerlein, Mech. Mater. **139**, 103200 (2019)
3. M. Aldén, H.L. Skriver, S. Mirbt, B. Johansson, Phys. Rev. Lett. **69**, 2296 (1992)
4. M. Aldén, S. Mirbt, H.L. Skriver, N.M. Rosengaard, B. Johansson, Phys. Rev. B **46**, 6303 (1992)
5. E.G. Moroni, G. Kresse, J. Hafner, J. Furthmüller, Phys. Rev. B **56**, 15629 (1997)
6. G.Y. Guo, H.H. Wang, Chin. J. Phys. **38**, 949 (2000)
7. G. Steinle-Neumann, Phys. Rev. B **77**, 104109 (2008)
8. C. Albrecht, A. Kumar, S. Xu, A. Hunter, I.J. Beyerlein, Phys. Rev. Mater. **5**, 043602 (2021)
9. S. Xu, Y. Su, L.T.W. Smith, I.J. Beyerlein, J. Mech. Phys. Solids **141**, 104017 (2020)
10. J. Kudrnovský, I. Turek, A. Pasturel, R. Tetot, V. Drchal, P. Weinberger, Phys. Rev. B **50**, 9603 (1994)
11. P. Söderlind, J.A. Moriarty, J.M. Wills, Phys. Rev. B **53**, 14063 (1996)
12. G. Steinle-Neumann, L. Stixrude, R.E. Cohen, Phys. Rev. B **60**, 791 (1999)
13. J.A. Yan, C.Y. Wang, S.Y. Wang, Phys. Rev. B **70**, 174105 (2004)
14. Y. Zaoui, H. Bendaoud, K.O. Obodo, L. Beldi, B. Bouhafs, J. Magn. Magn. Mater. **499**, 166312 (2020)
15. Y. Su, S. Xu, I.J. Beyerlein, J. Appl. Phys. **126**, 105112 (2019)
16. P. Söderlind, A. Landa, B. Sadigh, L. Vitos, A. Ruban, Phys. Rev. B **70**, 144103 (2004)
17. J.J. Ríos-Ramírez, J.F. Rivas-Silva, A. Flores-Riveros, Comput. Mater. Sci. **126**, 12 (2017)
18. K. Parlinski, J. łLażewski, P.T. Jochym, A. Chumakov, R. Rüffer, G. Kresse, EPL **56**, 275 (2001)
19. S.A. Khandy, D.C. Gupta, Int. J. Quantum Chem. **117**, e25351 (2017)
20. M.K. Butt, M. Yaseen, I.A. Bhatti, J. Iqbal, Misbah, A. Murtaza, M. Iqbal, M.M. AL-Anazy, M.H. Alhossainy, A. Laref, J. Mater. Res. Tech. **9**, 16488 (2020)
21. H. Rached, D. Rached, R. Khenata, A.H. Reshak, M. Rabah, Phys. Stat. Sol. (b) **246**, 1580 (2009)
22. S. Huang, W. Li, S. Lu, F. Tian, J. Shen, E. Holmström, L. Vitos, Scr. Mater. **108**, 44 (2015)
23. C. Niu, C.R. LaRosa, J. Miao, M.J. Mills, M. Ghazisaeidi, Nat. Comm. **9**, 1363 (2018)
24. E.G. Özdemir, Z. Merdan, Mater. Res. Express **6**, 086102 (2019)
25. Y. Su, S. Xu, I.J. Beyerlein, Model. Simul. Mater. Sci. Eng. **27**, 084001 (2019)

26. M.J. Mehl, D.A. Papaconstantopoulos, Phys. Rev. B **54**, 4519 (1996)
27. J.A. Rayne, B.S. Chandrasekhar, Phys. Rev. **122**, 1714 (1961)
28. H.M. Ledbetter, R.P. Reed, J. Phys. Chem. Ref. Data **2**, 531 (1973)
29. H.M. Ledbetter, R.L. Moment, Acta Metall. **24**, 891 (1976)
30. J.J. Adams, D.S. Agosta, R.G. Leisure, H. Ledbetter, J. Appl. Phys. **100**, 113530 (2006)
31. L. Vočadlo, GAd. Wijs, G. Kresse, M. Gillan, G.D. Price, Faraday Discuss. **106**, 205 (1997)
32. K.J. Caspersen, A. Lew, M. Ortiz, E.A. Carter, Phys. Rev. Lett. **93**, 115501 (2004)
33. X. Sha, R.E. Cohen, Phys. Rev. B **74**, 214111 (2006)
34. O. Kubaschwewski, *Iron-Binary Phase Diagrams* (Springer, Berlin, 1982)
35. H. Zhang, M.P.J. Punkkinen, B. Johansson, S. Hertzman, L. Vitos, Phys. Rev. B **81**, 184105 (2010)
36. A. Sutton, W. Hume-Rothery, Mag. J. Sci. Lond. Edinb. Dublin Philos. **46**, 1295 (1955)
37. Y. Yin, J. Zhang, Q. Tan, W. Zhuang, N. Mo, M. Bermingham, M.X. Zhang, Mater. Des. **162**, 24 (2019)
38. A. Zunger, S.H. Wei, L.G. Ferreira, J.E. Bernard, Phys. Rev. Lett. **65**, 353 (1990)
39. A. van de Walle, P. Tiwary, M. de Jong, D.L. Olmsted, M. Asta, A. Dick, D. Shin, Y. Wang, L.Q. Chen, Z.K. Liu, Calphad **42**, 13 (2013)
40. H. Warlimont, W. Martienssen, eds., Springer Handbook of Materials Data, Springer Handbooks, 2nd edn. (Springer International Publishing, 2018), ISBN 978-3-319-69741-3. https://www.springer.com/us/book/9783319697413
41. S. Xu, S.Z. Chavoshi, Y. Su, Comput. Mater. Sci. **202**, 110942 (2022)
42. A. Stukowski, Model. Simul. Mater. Sci. Eng. **18**, 015012 (2010)
43. J. von Pezold, A. Dick, M. Friák, J. Neugebauer, Phys. Rev. B **81**, 094203 (2010)
44. G. Kresse, J. Furthmüller, Phys. Rev. B **54**, 11169 (1996)
45. P.E. Blöchl, Phys. Rev. B **50**, 17953 (1994)
46. G. Kresse, D. Joubert, Phys. Rev. B **59**, 1758 (1999)
47. J.P. Perdew, K. Burke, M. Ernzerhof, Phys. Rev. Lett. **77**, 3865 (1996)
48. H.J. Monkhorst, J.D. Pack, Phys. Rev. B **13**, 5188 (1976)
49. M. Methfessel, A.T. Paxton, Phys. Rev. B **40**, 3616 (1989)
50. Y. Su, M. Ardeljan, M. Knezevic, M. Jain, S. Pathak, I.J. Beyerlein, Comput. Mater. Sci. **174**, 109501 (2020)
51. M. Born, K. Huang, *Dynamical Theory of Crystal Lattices* (Oxford University Press, New York, 1998)
52. S. Xu, E. Hwang, W.R. Jian, Y. Su, I.J. Beyerlein, Intermetallics **124**, 106844 (2020)
53. V.A. Bokov, N.A. Grigoryan, M.F. Bryzhina, V.V. Tikhonov, Phys. Stat. Solidi **28**, 835 (1968)
54. I. Solovyev, N. Hamada, K. Terakura, Phys. Rev. Lett. **76**, 4825 (1996)